NIH Public Access
Author Manuscript
Gene Ther. Author manuscript; available in PMC 2011 October 1.

Published in final edited form as:
Gene Ther. 2010 October ; 17(10): 1279–1287. doi:10.1038/gt.2010.69.

Local arterial nanoparticle delivery of siRNA for NOX2 knockdown to prevent restenosis in an atherosclerotic rat model

Jian-ming Li, MD, PhD[1], **Peter E. Newburger, MD**[2], **Matthew Gounis, PhD**[3], **Phong Dargon, MD**[1], **Xueqing Zhang, PhD**[2], and **Louis M. Messina, MD**[1]

[1]Department of Surgery, Division of Vascular Surgery, University of Massachusetts Medical School, Worcester, Massachusetts 01655, USA

[2]Departments of Pediatrics and Cancer Biology, University of Massachusetts Medical School, Worcester, Massachusetts 01655

[3]Department of Radiology, New England Center of Stroke Research, University of Massachusetts Medical School, Worcester, Massachusetts 01655

Abstract

Both atherosclerosis and arterial interventions induce oxidative stress mediated in part by NADPH oxidases that play a pivotal role in the development of neointimal hyperplasia and restenosis. For siRNA targeting of the NOX2 (Cybb) component of NADPH oxidase to prevent restenosis, gene transfer with viral vectors is effective, but raises safety issues in humans. We have developed a new approach using the amino-acid-based nanoparticle HB-OLD7 for local delivery of siRNA targeting NOX2 to the arterial wall. siRNA-nanoparticle complexes were transferred into regional carotid artery walls after angioplasty in an atherosclerotic rat model. Compared to angioplasty controls, Cybb gene expression (measured by quantitative RT-PCR) in the experimental arterial wall 2 weeks after siRNA was reduced >87%. The neointima to media area ratio was decreased >83% and lumen to whole artery area ratio was increased >89%. Vital organs showed no abnormalities and splenic Cybb gene expression showed no detectable change. Thus, local arterial wall gene transfer with HB-OLD7 nanoparticles provides an effective, non-viral system for efficient and safe local gene transfer in a clinically applicable approach to knockdown an NADPH oxidase gene. Local arterial knockdown of the Cybb gene significantly inhibited neointimal hyperplasia and preserved the vessel lumen without systemic toxicity.

Keywords

siRNA; NOX2; CYBB; gp91-phox; arterial restenosis; nanoparticles

Introduction

Atherosclerotic cardiovascular disease is a major cause of death and disability worldwide. Therapeutic interventions such as arterial angioplasty, stenting, and bypass have shown great short term success, but long term success is still limited by restenosis induced by neointimal hyperplasia and arterial remodeling. Drug-eluting stents have been proven to reduce restenosis

Correspondence to: Jian-ming Li, MD, PhD. Department of Surgery, Division of Vascular Surgery, University of Massachusetts Medical School. 55 Lake Avenue North, Worcester, MA 01655. Phone# 508-856-5511. Fax# 508-334-7810. jianming.li@umassmed.edu .

Conflict of Interest
The authors declare no conflict of interest.

NIH-PA Author Manuscript
NIH-PA Author Manuscript
NIH-PA Author Manuscript

NIH-PA Author Manuscript

NIH-PA Author Manuscript

NIH-PA Author Manuscript

in selected populations compared with bare metal stents in relatively short-term studies.[1–3] However, concerns about drug-eluting stents have developed over longer periods of follow-up, including altered vascular healing with incomplete vessel wall and stent re-endothelialization, late thrombus formation, restenosis, and occurrence of myocardial infarction and death.[4–8] Recent systematic reviews, large-scale registry studies, and a meta-analysis of 38 trials (18,023 patients) with a follow-up to 4 years, demonstrated similar rates of overall mortality and myocardial infarction rates for patients treated with either drug-eluting or bare-metal stents.[9] Reactive oxygen species (ROS) activate cell proliferation and are functionally involved in the development of arterial stenosis following balloon angioplasty. During inflammation, these molecules are generated by the phagocyte NADPH oxidase, a multi-component membrane-bound enzyme complex that includes, as a functionally critical component, the *CYBB* gene product gp91-phox, also termed NOX2. The NOX family includes NOX1, NOX2, NOX3, NOX4, NOX5, DUOX1, and DUOX2. All NOX enzymes generate ROS, including oxygen radicals (such as superoxide, O_2^-) and nonradicals (such as hydrogen peroxide, H_2O_2) that are involved not only in cellular damage and killing of pathogens, but also in a large number of reversible regulatory processes in virtually all cells and tissues.[10–13] In the vascular wall, superoxide anion mediates oxidative damage in atherosclerosis, and macrophage NOX2 appears to be the major oxidase affecting intimal smooth muscle cells (SMC).[14] NADPH oxidase also plays a potent role in enhancing intima-media thickness in children with hypercholesterolemia.15

NADPH oxidase deficiency significantly reduces atherosclerosis in apoE knockout mice, and atherosclerosis can be attenuated by limiting superoxide generation in both macrophages and vessel wall cells.[16] We have found, by microarray analysis that Cybb (NOX2) and Dpt (encoding the extracellular matrix protein dermatopontin) were the genes most up-regulated by inflammation in neointima at 4 days, 7 days and 14 days after balloon angioplasty.[17] Inhibition of NADPH oxidase with neutralizing antibody or peptide has been shown to decrease neointimal formation after arterial injury.[18,19]

Therapeutic knockdown of gene expression has been achieved by RNA inhibition (RNAi) from constructs expressed from viral vectors. For example, virus-mediated transfer of genes or siRNA for inhibition of neointimal hyperplasia in rats or rabbits has been reported, using replication-defective adenovirus-mediated knockdown of forkhead transcription factor genes to inhibit cell growth and cell cycle progression [20], complexed atelocollagen with siRNA targeting a heparin-binding growth factor Midkine 21, and lentiviral delivery of siRNA targeting an extracellular matrix-associated protein CCN1 22. Viral transfer is effective, but also raises safety issues in humans, including insertional mutagenesis leading to malignancy. 23

To address these limitations, we have developed a new approach using non-viral nanoparticles locally delivering siRNA. We hypothesized that nanoparticle delivery of siRNA to knockdown NOX2 expression in the carotid artery wall after balloon angioplasty would prevent neointimal hyperplasia in a rat model of hypercholesterolemia-induced atherosclerosis.

Results

Nanoparticle-Mediated siRNA Transfer in vitro

Figure 1 shows siGLO transfected into SMC cytoplasma with HB-OLD7 vector as red dots around the cell nucleus at 1, 2, 6 and 18 days, as detected by longitudinal spinning disk confocal microscopy. siGLO was transfected into all the cells after 24 hr, and carried into the daughter cells, as seen in the day 18 image.

NIH-PA Author Manuscript

NIH-PA Author Manuscript

NIH-PA Author Manuscript

Mouse Experiments—After 1, 3 and 4 days tail vein injection of siGLO and HB-OLD7 complex the mice were scanned under a Xenogen® IVIS™100 imaging system. Organ cryosection slide images (Supplemental figure 1) showed that siGLO (red dots) were seen in the vital organs (liver, spleen, kidney, lung, heart, and brain) and leg and thigh muscles. No evidence of transfection was found in the carotid artery cross sections (image not shown). The percentages of siGLO-positive organ cells, quantified using MetaMorph software, version 7.6.3., are presented in Table1.

Images of fluorescence staining for NOX2 in isolated mouse spleen phagocytes 3 days after tail vein injection of nanoparticles alone or nanoparticle-siCybb complex are shown in Supplemental figure 2. NOX2 was expressed in 12.65% of spleen phagocytes in mice treated with the empty nanoparticle control, compared to 9.91% in mice receiving nanoparticle-siCybb complex, a 27.4% decrease.

The mouse spleen cryo-slides were also double immuno-stained for NOX2 and the phagocyte marker CD11b (Supplemental figure 3). Quantification of 10 images of each group using IMAGE-PRO PLUS software showed that the proportion of NOX2 positive phagocytes in the nanoparticle-siCybb complex-treated mice decreased 60% compared to empty nanoparticle group.

Western blots of protein expression in three mice spleens are shown in Supplemental figure 4. NOX2 expression in spleen after IV administration of nanoparticle-siCybb complex was 30% lower than that seen after administration of nanoparticles alone.

Atherosclerotic Rat Model

Hematoxylin and eosin staining demonstrated calcium deposits in the ascending thoracic aorta after 6 weeks and atherosclerotic plaques formed in the aortas after 10 to 12 weeks (Figure 2) of the high-fat diet. Hence, we conducted the rat experiments 10–12 weeks after the initiation of the diet. Compared to pre-high-fat diet, blood cholesterol, triglycerides, and LDL were elevated after 6 weeks high-fat chow ($P < 0.001$). There were no significant changes in HDL or VLDL. Liver functions (AST and ALT) and kidney function (creatinine) did not show significant changes after high-fat chow. Blood granulocytes, monocytes and lymphocytes were elevated at 2 weeks after surgery, probably in response to surgical injury, with no significant effect between control and experimental groups.

Effects of Nanoparticle-siSTABLE-Cybb Complex Transfer

In order to experiment the feasibility of using nanoparticles to deliver siRNA into the local arterial wall, we test the route of transferring the HB-OLD7 and siGLO complex (red fluorescence) to the carotid artery by luminal and adventitial approaches after balloon angioplasty. Four days after delivery by the local adventitia approach, siGLO (red dots) was detectable throughout the arterial wall by fluorescent microscopy with suppression of autofluoresence (figure 3a) and by high-resolution fluorescent confocal microscopy (figure 3b). We tested an alternative approach via the regional vessel lumen by introducing nanoparticle-siGLO complex into the arterial lumen after balloon angioplasty, with the blood circulation interrupted for 25 min using non-traumatic micro-vascular clamps. After 4 days there was no evidence of siGLO-Dy547 into the arterial wall. (images not shown) Therefore, the peri-adventitial route of siRNA transfer was used in further studies.

Nanoparticle HB-OLD7-siSTABLE-Cybb (siCybb) complex were delivered to the adventitia of the left carotid artery after balloon angioplasty in the atherosclerotic rat model. Bilateral carotid arteries and spleen were removed two weeks later and analyzed by qRT-PCR and western blot to evaluate the effectiveness of siRNA knockdown of NOX2. In addition, the

NIH-PA Author Manuscript

NIH-PA Author Manuscript

NIH-PA Author Manuscript

functional consequences of NOX2 knockdown were analyzed by histological morphometric analysis of intimal to media area ratio and luminal to whole artery area ratio.

mRNA Expression—Quantitative real time RT-PCR (qRT-PCR) was performed to measure mRNA expression in the rat carotid artery and the spleen. Levels of target gene (Cybb) expression were normalized over the internal control gene rps6 (ribosomal protein s6). As shown in Figure 4a, in the carotid artery, nanoparticle delivery of siCybb reduced Cybb expression by 87.1%, 87.3% and 88.6% relative to angioplasty only, vector control, and siControl groups, respectively (n=6). No systemic change in Cybb expression was observed in the spleen after local transfer of siCybb in the carotid artery (figure 4b).

There were no changes in the levels of NOX4 mRNA expression in the rat carotid artery after angioplasty with and without siCybb-nanoparticle complex transfer are shown in Supplemental Figure 5.

Protein Expression—Immunoblots were probed with antibodies to NOX2 and CD11b (phagocytes marker), detected by chemiluminescence. As shown in figure 5a, NOX2 protein expression in the carotid artery, standardized to CD11b and to α-tubulin proteins after nanoparticle-mediated siCybb transfer, was decreased by 71.9%, 73.1% and 70.2% relative to angioplasty only, empty nanoparticle, and siControl groups (n=5). Normalization to CD11b was used to control for differing numbers of phagocytes in the samples. In the spleen there were no significant differences observed between the groups in NOX2 protein levels.(Figure 5b).

ROS Production—Figure 6 presents cryo-sections of rat carotid arteries stained with dihydroethidium (DHE), an indicator of superoxide anions, at two weeks after siRNA delivery. Superoxide (red stain) is evident in thickened neointima and adventitia in the nanoparticle vector control artery. Notably, in the nanoparticle-siCybb complex treated arteries, neointima formation was inhibited and very little superoxide was detectable in the arterial wall (Figure 6). ROS expression was quantitated with IMAGE-PRO PLUS 6.2 software. After siCybb transfer, the proportion of ROS-positive arterial cells was decreased 89.7% and 72.6%, compared to transfer of nanoparticles alone.

Neointima Formation—Cryo-sections of the carotid arteries were stained with hematoxylin and eosin and the areas of neointimal hyperplasia and vessel lumen were measured by digital imaging planimetry. As shown in figure 7, neointima formation was dramatically inhibited, with intimal to media area (I/M) ratio decreased more than 83%. Lumen areas were significantly preserved, with luminal to whole artery area (L/W) ratio increased more then 89% compared to the angioplasty control group (n=6).

Discussion

Arterial injury in atherosclerotic arteries leads to the infiltration and activation of leukocytes, with induction of local ROS production, as well as cytokine and chemokine release, that accelerate formation of neointimal hyperplasia.[24] Our laboratory has shown that inflammatory cells including monocytes and neutrophils adhere and infiltrate into the artery wall after angioplasty in rat carotid artery [17], non-atherosclerotic rabbit [25] and atherosclerotic rabbit models [26]. ROS are generated in vascular cells by NADPH oxidases, uncoupled endothelial nitric oxide synthase producing superoxide rather than nitric oxide, and other enzymatic sources, or as byproducts of mitochondrial respiration.[27] The most active of these systems, the phagocyte NADPH oxidase, is a multi-component membrane-bound enzyme complex that belongs to the NOX family. NOX2 is a critical functional component of the phagocyte NADPH oxidase. All NOX enzymes generate ROS, including oxygen radicals (such as superoxide,

NIH-PA Author Manuscript

NIH-PA Author Manuscript

NIH-PA Author Manuscript

O_2^-) and non-radicals, (such as hydrogen peroxide, H_2O_2), that are either oxidizing agents or are easily converted into radicals. ROS are involved not only in cellular damage and killing of pathogens, but also in a large number of reversible regulatory processes in virtually all cells and tissues.[10–13] ROS play a critical role in vascular injury. In the vascular wall, superoxide anion mediates oxidative damage in atherosclerosis, and macrophage NOX2 appears to be the major oxidase affecting intimal SMC.[14]

In the current study, siRNA targeting NOX2 was successfully transferred to the local arterial wall using a new nanoparticle vector, HB-OLD7, delivered via an adventitia approach at 2 weeks after angioplasty in atherosclerotic rats. Transfection of fluorescent-tagged siRNA by HB-OLD7 carrier into rat arterial SMC persisted in the original transfected cells and daughter cells for up to 18 days.

Nanoparticle delivery of siRNA to Cybb, the gene encoding NOX2, resulted in the inhibition of neointimal hyperplasia and preserved luminal area by approximately 90% at 2 weeks after arterial intervention. Our previous studies showed that neointimal hyperplasia reaches a plateau at 2–4 weeks after surgery in rat [17], rabbit [25, 26] and pig models [28]. However, the accelerated development of hyperplasia in animals is in contrast to the usual time course for the development of neointimal hyperplasia in humans, which ranges from months to a year or more. Ongoing studies of the long term effects of siRNA silencing are evaluating these measurements at times up to 18 months.

The absence of a similar effect from delivery of negative control construct indicates that the observed biochemical and histological changes resulted from NOX2 silencing, not from the alternative, non-specific mechanism of Toll-like receptor 3 activation.[29,30]

Phagocyte ROS generated by NOX2 also provide beneficial microbicidal activity critical to host defense against bacteria and fungi.31 In theory, systemic delivery of the nanoparticle siRNA-Cybb complex could silence Cybb expression and impair host defense against these organisms, as in the hereditary disorder chronic granulomatous disease (CGD).32 However, clinically significant impairment of host defense does not occur unless NOX2 activity falls below 10% of normal: mutations leading to retention of 5–10% normal activity lead to clinically milder “variant” CGD, and carriers of X-linked CGD are asymptomatic unless random X inactivation produces a distribution of >90% abnormal cells.33 In our studies with systemic (intravenous) administration of nanoparticle siRNA-Cybb complex in mouse, spleen phagocyte Cybb expression fell only 30%. Far less systemic distribution would be expected from local administration of the nanoparticles to the arterial adventitia. Indeed, as shown in figure 5b and figure 6b, there were no detectable changes in phagocyte Cybb gene expression or NOX2 protein levels in splenic phagocytes.

Overall, the present studies show that siRNA delivered by the nanoparticle vector HB-OLD7 can be tranfected into arterial SMC in culture, and transferred into a blood vessel wall *in vivo*. Systemic and arterial luminal routes of administration did not effectively transfer siRNA into the arterial wall. However, a local arterial adventitial approach successfully transferred the siCybb-nanoparticle complex into the rat common carotid artery after angioplasty and significantly silenced regional Cybb gene expression, inhibited intimal hyperplasia and preserved the artery lumen area. Liver and kidney functions and histology showed no change after local arterial siRNA transfer. Nanoparticle-mediated local arterial delivery of siCybb resulted in no abnormal liver or kidney function or histology, nor any changes in spleen histology, Cybb transcript levels, or NOX2 protein expression. The siRNA-Cybb signaling pathway are under further investigation.

The peri-adventitia delivery approach would be clinically applicable in the open vascular reconstructive surgery, such as coronary artery bypass or carotid artery endarterectomy, which

NIH-PA Author Manuscript

NIH-PA Author Manuscript

NIH-PA Author Manuscript

remain common procedures for the treatment of coronary and carotid artery atherosclerotic stenosis.[34,35] Delivery of siRNA to the adventitia is both practically convenient in open vascular surgery, and pathophysiologically appropriate. [36] In recent years, evidence has emerged indicating that the vascular adventitia is activated early in a variety of cardiovascular diseases and that NADPH oxidase-derived ROS from the adventitia play an important role in the initiation and progression of vascular inflammation, arterial remodeling and intimal hyperplasia.

Materials and Methods

siRNA and Nanoparticle Formation

siGLO-Dy547 is a non-targeting siRNA tagged with red fluorescence dye Dy547. siControl is a non-targeting siRNA control, which targets luciferase. siGLO-Dy547, siControl and siSTABLE-Cybb (siCybb) are stability-enhanced siRNA for *in vivo* study constituted by Dharmacon RNAi Technologies (Lafayette, CO. USA), average MW 13,300 g/mol. siSTABLE-Cybb, which targets CYBB (GenBank accession NM_023965), represents an siRNA pool designed with the “inVIVO SMARTpool” technique (Dharmacon) that incorporates a multi-component algorithm to identify siRNAs with a high probability of potent and specific silencing. SMARTpool reagents combine four SMART selection-designed siRNA into a single pool. The siRNAs were targeted to the Cybb open reading frame, and follow a leader AA, but AA dinucleotide is not in part of the 19-nt sequence core. The sequences of the siSTABLE-Cybb siRNAs are: ACGAUGAGCCUAAAUAUAA, GCAGGGACACGCAUGCUUU, GCUACAACAUCUACCUUAC, and UCAAGACCAUUGCAAGUCA; these target Cybb sequences in exons 2, 11, 11, and 12, respectively.

HB-OLD7 nanoparticles were developed by Dr. Tariq Rana’s laboratory as previously described. The lysine-based nanoparticles feature surface modifications incorporating oleic acid, a monounsaturated omega-9 fatty acid, as a functional group, MW 5,798 g/mole. HB-OLD7 binds to siRNA through electrostatic interaction and forms nanoparticles with diameter less than 200 nm. The functionalized nanoparticle–siRNA complexes initiate contacts with the cell membrane for entry and intracellular release of the siRNA. [37,38]

Primers for rat and mouse Cybb, NOX4 and internal control rps6 oligonucleotides were obtained from Operon (Huntsville, AL, USA). Antibodies to NOX2 and CD11b were from BD Biosciences (San Jose, CA, USA).

In Vitro Experiment

To determine the efficacy of siRNA transfection, siGLO-Dy547 was used to transfect smooth muscle cells (SMC) using HB-OLD7 as a vector. Rat descending thoracic aorta SMC were explanted and passages 2–3 were seeded onto a 35mm glass culture dishes (MatTek, Ashland, MA, USA) in Waymouths’ MB752/1 medium plus L-Glutamine (GIBCO, Invitrogen). The final concentration of siGLO in 35mm dish was 100 nmol/L with 1:1 siGLO to siRNA weight ratio. The efficacy of transfection was monitored using a CSU10B Spinning Disk Confocal System (Solamere Technology Group, Salt Lake City, UT. USA) attached to a Nikon TE2000-E2 automated inverted microscope (Melville, NY. USA) at 1, 2, 6, and 18 days after transfection.

Mouse Experiments

All animal experiments were conducted with the approval of the University of Massachusetts Medical School Institutional Animal Care and Use Committee.

NIH-PA Author Manuscript

NIH-PA Author Manuscript

NIH-PA Author Manuscript

To track siRNA biodistribution following intravenous administration, siGLO–HB-OLD7complex was administrated via intravenous injection in wild type C57BL/6J mice. The siGLO-Dy547 (1mg/kg body weight) and HB-OLD7 complex (1:8 W/W ratio) [37] was injected through the tail vein. After 1, 3, and 4 days the mice were scanned by a Xenogen® IVIS™100 imaging system (Caliper LifeSciences, Hopkinton MA, USA), then sacrificed. The carotid arteries, vital organs, and thigh muscles (vastus lateralis and biceps femoris) and leg muscle (gastrocnemius) were removed and cryo-sectioned. siGLO distribution in the organs was imaged by fluorescence microscopy (Olympus IX-70, Olympus America, Inc. Center Valley, PA. USA) and quantified with MetaMorph software, version 7.6.3 (MDS Analytical Technologies, Dowingtown, PA. USA).

Spleen monocytes and macrophages (Mono/Macro) were harvested using BD Falcon Cell Strainer, 70um (BD Biosciences, San Jose, CA. USA) and assayed for NOX2 expression 3 days after HB-OLD7 alone or siCybb-HB-OLD7 complex intravenous administration. Equal amount of cells were seeded into 8-chamber cover slide (Lab-Tek /Chamber Slide, Cat#177445, Nalge Nunc International, Rochester, NY. USA) for NOX2 immunostaining.

Rat Experiments

Atherosclerosis induction and arterial balloon injury—White Sprague Dawley rats (male, 400± 25g body weight) were administered vitamin D_3 60,000 IU/100g body weight intra-peritoneally [39] and fed with a high fat chow containing 21% fat and 0.15% cholesterol (Cat# 5TKW, TestDiet Co., Richmond, IN. USA). The aortas were subsequently removed weekly after 3–12 weeks of feeding high fat chow for histological evaluation of the atherosclerosis status. There was calcium deposition in the ascending aorta at 6 weeks, and obvious plaques in the inner layer of the ascending and descending aortas beginning at 10 weeks. Based on these longitudinal observations, the rats were allowed to maintain this diet up until 10–12 weeks at which point balloon angioplasty of left common carotid artery was performed. The rats were fed with regular chow after surgery.

Analgesics Depodur® (Liposome-encapsulated morphine) 2.8 mg/kg, and glycopyrrolate 0.02 mg/kg, an anticholinergic drug to maintain heart rate and decrease salivation, were administered subcutaneously before induction of anesthesia. General anesthesia was induced in a 5% isoflurane chamber, and maintained with 1%-2% isoflurane inhalation through a cone-mask. LCA was injured using a 2F arterial embolectomy catheter (Fogarty®, Edwards Lifesciences™, U.S.A) introduced through the external carotid artery under temporary clamping of the proximal common carotid and internal carotid arteries. The balloon was inflated and withdrawn three times to expand the artery and denude endothelium.[17]

The total volume of nanoparticle-siRNA complex was 100μl. The weight ratios of nanoparticle to siGLO (5.3μg) were first tested from 20:1to 200:1 for tracing siRNA-Dy547 (red) under fluorescent microscope at 4 days after transfer. Red dots were seen throughout the regional arterial wall at all ratios above 80:1. Hence, the nanoparticle:siRNA (93 μg) ratio of 100:1 was used in all subsequent experiments.

For the rat experiments, siGLO, siControl, or siCybb was encapsulated with HB-OLD7 at 100:1 weight ratio at 22°C for 20 min to 1 h prior to use. Nanoparticles or nanoparticles encapsulating were one of these siRNAs applied circumferentially to the adventitia of LCA after balloon angioplasty.

Blood was drawn via the retro-orbital route prior to the high fat diet, on the day of surgery, and at termination (two weeks after surgery) for measurements of serum lipids, aspartate transaminase (AST), alanine transaminase (ALT) and creatinine. Blood cell numbers and distribution were also measured.

NIH-PA Author Manuscript

NIH-PA Author Manuscript

NIH-PA Author Manuscript

There were four animal groups in each trial: three control groups (angioplasty only, nanoparticle control, and nanoparticle-siControl complexes) and a treatment group that received siCybb.

Fluorescent-labeled siRNA was detected in the arterial wall by fluorescent microscopy (Olympus IX) and high-resolution fluorescent confocal microscopy Leica DM IRBE (Leica Microsystems Inc., Bannockburn IL, USA). The images were later processed to remove autofluorescence with the Nuance FX multispectral imaging system (CRI Inc., Woburn, MA, U.S.A) and Nuance software.

In vivo Cybb (NOX2) knockdown—Two weeks after angioplasty and treatment with empty nanoparticles or nanoparticles delivering siControl or siSTABLE-Cybb, bilateral carotid arteries and spleens were harvested into RNAlater (an RNA stabilization solution for tissue collection; Ambion, Austin, TX. U.S.A) for later study. The specimens were evaluated for the molecular effects of NOX2 knockdown and for ROS production with immunofluorescence staining. Western immunoblot and qRT-PCR were used for quantification of NOX2, as well as for NOX4 (an arterial smooth muscle cell oxidase).

Quantitative RT-PCR was used to detect mRNA expression levels of NOX2 and NOX4 relative to the internal control gene rps6 in the rat carotid artery, and of NOX2 in spleen. The samples were mechanically homogenized with POLYTRON PT 2100 (Kinematica, Inc., subsidiary of Kinematica, AG (Lucerne, Switzerland), Bohemia, NY. USA). Total RNA was extracted with TRIzol (Invitrogen). First strand cDNAs were synthesized with an anchored oligo(dT) primer using Superscript™ III First strand synthesis Super MIX for qRT-PCR (Invitrogen). Real-time PCR was performed on a Realplex^2 Mastercycler epgradient S (Eppendorf North America, Westbury, NY. USA). The relative standard curve derived from serial dilutions of sample first strand cDNA was used for quantification. Levels of target gene expression for rat samples were normalized over the internal control gene rps6 .

Vascular smooth muscle cells express mRNA for NOX4, which shares approximately 39% identity to NOX2.[13] In order to determine the specificity of the NOX2 knockdown we also evaluated the expression of NOX4 mRNA in the same arterial specimens.

NOX2 protein knockdown was evaluated by immunofluorescence staining and western blot. Cryo-sections of the carotid arteries harvested at intervals after balloon angioplasty with and without siRNA treatment were double-stained with mouse monoclonal antibody to NOX2 and mouse anti-rat CD11b (BD Biosciences). Second antibodies used for NOX2 and CD11b were, respectively, FITC-conjugated AffiniPure goat anti mouse IgG (H+L) and Rhodamine Red-X-conjugated AffiniPure goat anti-mouse IgG (H+L) (Jackson ImmuResearch Laboratories, Inc. West Grove PA. USA).

For Western blotting, samples were homogenized in Cell Lysis Buffer (Cell Signaling Technology Inc., Danvers, MA. USA) supplemented with Protease Inhibitor Cocktail (Sigma-Aldrich, St. Louis, MO. USA). Sample proteins were separated on 10% precast polyacrylamide gels (Bio-Rad Laboratories, Hercules, CA. USA) and then electro-transferred to nitrocellulose (0.45um) membrane (Bio-Rad). The membranes were probed with each of the primary antibodies to NOX2 or CD11b (BD Biosciences). Signals were detected with Western Lighting Chemiluminescence Reagent Plus (PerkinElmer LAS, Inc., Waltham, MA. USA). Protein band intensity was quantified with ImageJ software.

Cryo-sections of the carotid artery samples were subjected to histochemical staining with dihydroethidium (DHE, Invitrogen Corp. Grand Island, NY. USA), an indicator of superoxide anions.

NIH-PA Author Manuscript

NIH-PA Author Manuscript

NIH-PA Author Manuscript

Histomorphometry—For histomorphometric measurements, bilateral carotid artery samples were retrieved after *in situ* perfusion with 0.9% saline and fixation with 4% paraformaldehyde at 110–120 mmHg pressure for 30 min. Samples were then kept in 4% paraformaldehyde for at least 48 hours. The artery samples were then cross-sectioned into proximal 1/3, middle1/3 and distal 1/3 segments and snap frozen with O.C.T. compound (Tissue-Tek, Sakuru Tinetek, USA, Inc). The cryo-sections were processed to 5um thickness and 10 sections for each segment for hematoxylin and eosin stain. Neointimal and luminal areas were measured with digital imaging planimetry using ImageJ software.

Detection of Systemic Silencing Effects—Spleen were retrieved along with bilateral carotid arteries from each animal at termination and evaluated for NOX2 expression with: 1. Double immunofluorescent staining for NOX2 and CD11b (phagocyte marker); 2. Western blot for NOX2 and CD11b proteins; 3. Quantitative RT-PCR for Cybb mRNA expression, and immunohistofluorescence staining. The liver and kidney were also retrieved for histological evaluation.

Statistical Analysis—The effects of treatment, and arterial segment were evaluated by analysis of variance (ANOVA) for mixed models.[40] In the presence of significant main or interaction effects, pairwise comparisons were performed using the Tukey-Kramer multiple comparisons procedure.41 The distributional characteristics of the outcome variables were assessed using the Kolmogorov-Smirnov goodness-of-fit test for normality on model residuals. All computations were performed using SAS 9.1.3 Proc Mixed and SPSS 14 statistical software. $P < 0.05$ is considered significant.

Supplementary Material

Refer to Web version on PubMed Central for supplementary material.

Acknowledgments

We thank Tariq M. Rana, PhD and Huricha Baigude, PhD, Burnham Institute for Medical Research, La Jolla, CA for providing nanoparticles and for helpful study discussions; Stephen Baker, MScPH, Senior Biostatistician, Department of Cell Biology and Information Resources for assistance of statistical analysis; Paul S. Furcinitti, PhD, Director of Digital Light Microscopy Core Facility for confocal microscopy and image analysis, and Jeffrey Nickerson, PhD, Department of Cell Biology, Director of Confocal Microscopy Core Facility, the University of Massachusetts Medical School.

Sources of Support: The Bugher Foundation (to J-M.L.), NIH grants R21AIAI079788 and R01DK54369 (to P.E.N.), R21EB007767 (to M.G.), R01HL075353 (to L.M.M.) and University of Massachusetts Medical School Chair Research Fund (to L.M.M.).

Non-standard Abbreviations and Acronyms

siGLO	(siGLO-Dy547)
siControl	(a non-targeting siRNA control, which targets luciferase)
siCybb	(siSTABLE targeting RNA Cybb)
LCA	(Left carotid artery)
SMC	(rat thoracic smooth muscle cells)
AST	(aspartate transaminase)
ALT	(alanine transaminase)

NIH-PA Author Manuscript

NIH-PA Author Manuscript

NIH-PA Author Manuscript

References

1. Morice MC, Serruys PW, Sousa JE, Fajadet J, Ban Hayashi E, Perin M, et al. A randomized comparison of a sirolimus-eluting stent with a standard stent for coronary revascularization. N Engl J Med 2002;346:1773–1780. [PubMed: 12050336]
2. Moses JW, Leon MB, Popma JJ, Fitzgerald PJ, Holmes DR, O'Shaughnessy C, et al. Sirolimus-eluting stents versus standard stents in patients with stenosis in a native coronary artery. N Engl J Med 2003;349:1315–1323. [PubMed: 14523139]
3. Grube E, Silber S, Hauptmann KE, Mueller R, Buellesfeld L, Gerckens U, et al. TAXUS I: six- and twelve-month results from a randomized, double-blind trial on a slow-release paclitaxel-eluting stent for de novo coronary lesions. Circulation 2003;107:38–42. [PubMed: 12515740]
4. Austin D, Oldroyd KG, Holmes DR Jr, Rihal CS, Galbraith PD, Ghali WA, et al. Drug-eluting stents: a study of international practice. Am Heart J 2009;158:576–584. [PubMed: 19781417]
5. Windecker S, Juni P. Safety of drug-eluting stents. Nat Clin Pract Cardiovasc Med 2008;5:316–328. [PubMed: 18414453]
6. Rosamond W, Flegal K, Furie K, Go A, Greenlund K, Haase N, et al. Heart disease and stroke statistics--2008 update: a report from the American Heart Association Statistics Committee and Stroke Statistics Subcommittee. Circulation 2008;117:e25–e146. [PubMed: 18086926]
7. van der Hoeven BL, Pires NM, Warda HM, Oemrawsingh PV, van Vlijmen BJ, Quax PH, et al. Drug-eluting stents: results, promises and problems. Int J Cardiol 2005;99:9–17. [PubMed: 15721493]
8. Muni NI, Gross TP. Problems with drug-eluting coronary stents--the FDA perspective. N Engl J Med 2004;351:1593–1595. [PubMed: 15483274]
9. Stettler C, Wandel S, Allemann S, Kastrati A, Morice MC, Schomig A, et al. Outcomes associated with drug-eluting and bare-metal stents: a collaborative network meta-analysis. Lancet 2007;370:937–948. [PubMed: 17869634]
10. Mohazzab KM, Kaminski PM, Wolin MS. NADH oxidoreductase is a major source of superoxide anion in bovine coronary artery endothelium. Am J Physiol 1994;266:H2568–H2572. [PubMed: 8024019]
11. Jones SA, O'Donnell VB, Wood JD, Broughton JP, Hughes EJ, Jones OT. Expression of phagocyte NADPH oxidase components in human endothelial cells. Am J Physiol 1996;271:H1626–H1634. [PubMed: 8897960]
12. Irani K, Xia Y, Zweier JL, Sollott SJ, Der CJ, Fearon ER, et al. Mitogenic signaling mediated by oxidants in Ras-transformed fibroblasts. Science 1997;275:1649–1652. [PubMed: 9054359]
13. Bedard K, Krause KH. The NOX family of ROS-generating NADPH oxidases: physiology and pathophysiology. Physiol Rev 2007;87:245–313. [PubMed: 17237347]
14. Kalinina N, Agrotis A, Tararak E, Antropova Y, Kanellakis P, Ilyinskaya O, et al. Cytochrome b558-dependent NAD(P)H oxidase-phox units in smooth muscle and macrophages of atherosclerotic lesions. Arterioscler Thromb Vasc Biol 2002;22:2037–2043. [PubMed: 12482831]
15. Martino F, Loffredo L, Carnevale R, Sanguigni V, Martino E, Catasca E, et al. Oxidative stress is associated with arterial dysfunction and enhanced intima-media thickness in children with hypercholesterolemia: the potential role of nicotinamide-adenine dinucleotide phosphate oxidase. Pediatrics 2008;122:e648–e655. [PubMed: 18762499]
16. Vendrov AE, Hakim ZS, Madamanchi NR, Rojas M, Madamanchi C, Runge MS. Atherosclerosis is attenuated by limiting superoxide generation in both macrophages and vessel wall cells. Arterioscler Thromb Vasc Biol 2007;27:2714–2721. [PubMed: 17823367]
17. Li JM, Zhang X, Nelson PR, Odgren PR, Nelson JD, Vasiliu C, et al. Temporal evolution of gene expression in rat carotid artery following balloon angioplasty. J Cell Biochem 2007;101:399–410. [PubMed: 17171642]
18. Kanellakis P, Nestel P, Bobik A. Angioplasty-induced superoxide anions and neointimal hyperplasia in the rabbit carotid artery: suppression by the isoflavone trans-tetrahydrodaidzein. Atherosclerosis 2004;176:63–72. [PubMed: 15306176]
19. Jacobson GM, Dourron HM, Liu J, Carretero OA, Reddy DJ, Andrzejewski T, et al. Novel NAD(P)H oxidase inhibitor suppresses angioplasty-induced superoxide and neointimal hyperplasia of rat carotid artery. Circ Res 2003;92:637–643. [PubMed: 12609967]

NIH-PA Author Manuscript NIH-PA Author Manuscript NIH-PA Author Manuscript

20. Abid MR, Yano K, Guo S, Patel VI, Shrikhande G, Spokes KC, et al. Forkhead transcription factors inhibit vascular smooth muscle cell proliferation and neointimal hyperplasia. J Biol Chem 2005;280:29864–29873. [PubMed: 15961397]
21. Banno H, Takei Y, Muramatsu T, Komori K, Kadomatsu K. Controlled release of small interfering RNA targeting midkine attenuates intimal hyperplasia in vein grafts. J Vasc Surg 2006;44:633–641. [PubMed: 16950446]
22. Matsumae H, Yoshida Y, Ono K, Togi K, Inoue K, Furukawa Y, et al. CCN1 knockdown suppresses neointimal hyperplasia in a rat artery balloon injury model. Arterioscler Thromb Vasc Biol 2008;28:1077–1083. [PubMed: 18388330]
23. Jin S, Ye K. Nanoparticle-mediated drug delivery and gene therapy. Biotechnol Prog 2007;23:32–41. [PubMed: 17269667]
24. Libby P, Ridker PM, Maseri A. Inflammation and atherosclerosis. Circulation 2002;105:1135–1143. [PubMed: 11877368]
25. Li JM, Singh MJ, Itani M, Vasiliu C, Hendricks G, Baker SP, et al. Recombinant human thrombomodulin inhibits arterial neointimal hyperplasia after balloon injury. J Vasc Surg 2004;39:1074–1083. [PubMed: 15111864]
26. Li JM, Eslami MH, Rohrer MJ, Dargon P, Joris I, Hendricks G, et al. Interleukin 18 binding protein (IL18-BP) inhibits neointimal hyperplasia after balloon injury in an atherosclerotic rabbit model. J Vasc Surg 2008;47:1048–1057. [PubMed: 18455646]
27. Mueller CF, Laude K, McNally JS, Harrison DG. ATVB in focus: redox mechanisms in blood vessels. Arterioscler Thromb Vasc Biol 2005;25:274–278. [PubMed: 15514203]
28. Wong G, Li JM, Hendricks G, Eslami MH, Rohrer MJ, Cutler BS. Inhibition of experimental neointimal hyperplasia by recombinant human thrombomodulin coated ePTFE stent grafts. J Vasc Surg 2008;47:608–615. [PubMed: 18295112]
29. Kleinman ME, Yamada K, Takeda A, Chandrasekaran V, Nozaki M, Baffi JZ, et al. Sequence- and target-independent angiogenesis suppression by siRNA via TLR3. Nature 2008;452:591–597. [PubMed: 18368052]
30. Cho WG, Albuquerque RJ, Kleinman ME, Tarallo V, Greco A, Nozaki M, et al. Small interfering RNA-induced TLR3 activation inhibits blood and lymphatic vessel growth. Proc Natl Acad Sci U S A 2009;106:7137–7142. [PubMed: 19359485]
31. Babior BM. NADPH oxidase. Curr Opin Immunol 2004;16:42–47. [PubMed: 14734109]
32. Malech HL, Hickstein DD. Genetics, biology and clinical management of myeloid cell primary immune deficiencies: chronic granulomatous disease and leukocyte adhesion deficiency. Curr Opin Hematol 2007;14:29–36. [PubMed: 17133097]
33. Robbins M, Judge A, Ambegia E, Choi C, Yaworski E, Palmer L, et al. Misinterpreting the therapeutic effects of siRNA caused by immune stimulation. Hum Gene Ther. 2008
34. Daemen J, Boersma E, Flather M, Booth J, Stables R, Rodriguez A, et al. Long-term safety and efficacy of percutaneous coronary intervention with stenting and coronary artery bypass surgery for multivessel coronary artery disease: a meta-analysis with 5-year patient-level data from the ARTS, ERACI-II, MASS-II, and SoS trials. Circulation 2008;118:1146–1154. [PubMed: 18725490]
35. Investigators ICSS. Carotid artery stenting compared with endarterectomy in patients with symptomatic carotid artery stenosis (International Carotid Stenting Study):an intrim analysis of a randomised controlled trial. Lancet. 2010
36. Csanyi G, Taylor WR, Pagano PJ. NOX and inflammation in the vascular adventitia. Free Radic Biol Med 2009;47:1254–1266. [PubMed: 19628034]
37. Rana TM. Illuminating the silence: understanding the structure and function of small RNAs. Nat Rev Mol Cell Biol 2007;8:23–36. [PubMed: 17183358]
38. Baigude H, McCarroll J, Yang CS, Swain PM, Rana TM. Design and creation of new nanomaterials for therapeutic RNAi. ACS Chem Biol 2007;2:237–241. [PubMed: 17432823]
39. Yang PY, Rui YC, Lu L, Li TJ, Liu SQ, Yan HX, et al. Time courses of vascular endothelial growth factor and intercellular adhesion molecule-1 expressions in aortas of atherosclerotic rats. Life Sci 2005;77:2529–2539. [PubMed: 16005023]
40. Elashoff, JD. nQuery Advisor Release 6.0 User's Guide. Los Angeles, CA: Statistical Solution, Inc; 2005.

41. McLean RA, Sanders WL, Stroup WW. A unified approach to mixed linear models. Am Stat 1991;45:54–64.

NIH-PA Author Manuscript

NIH-PA Author Manuscript

NIH-PA Author Manuscript

NIH-PA Author Manuscript

NIH-PA Author Manuscript

NIH-PA Author Manuscript

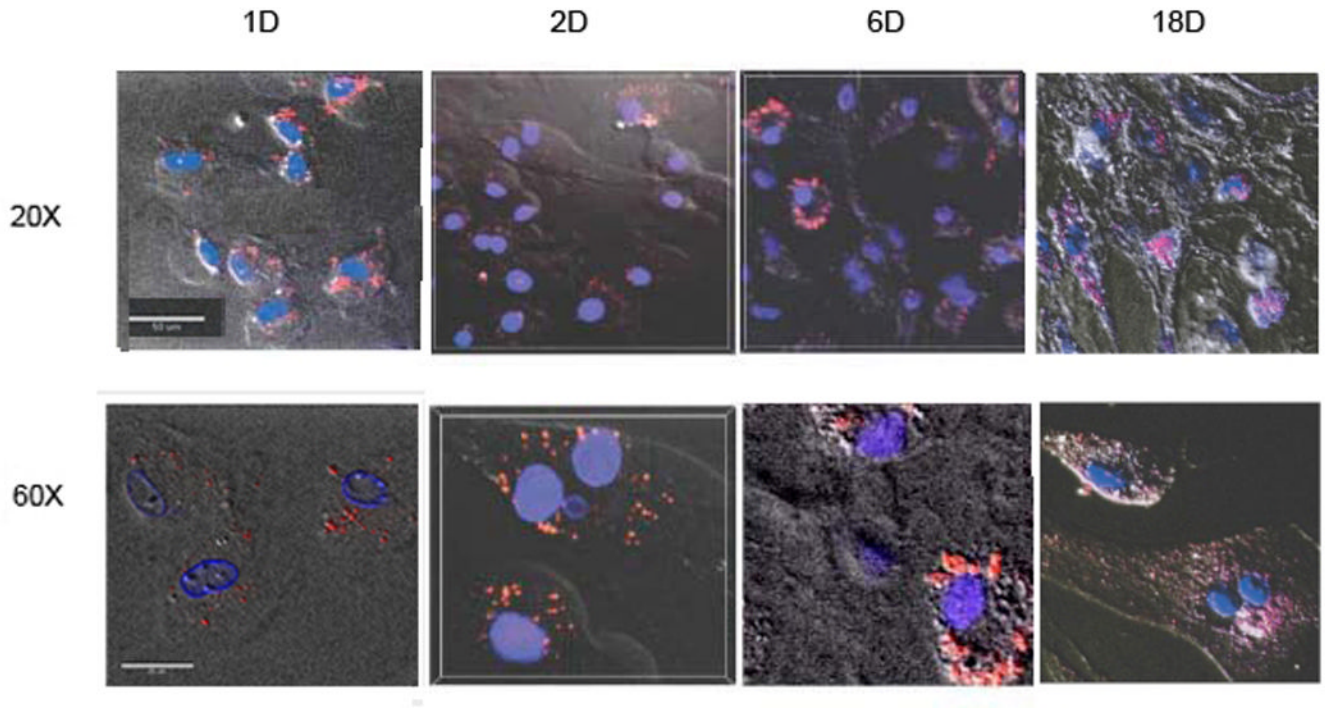

Figure 1. siGLO-nanoparticle complex transfection in rat thoracic aorta SMC in culture

Spinning disk fluorescent confocal microscopy at days 1 to 18 after transfection shows intracellular siRNA-Dy547 (siGLO, red dots). Scale bar: 20× 50μm; 60× 25 μm

NIH-PA Author Manuscript

NIH-PA Author Manuscript

NIH-PA Author Manuscript

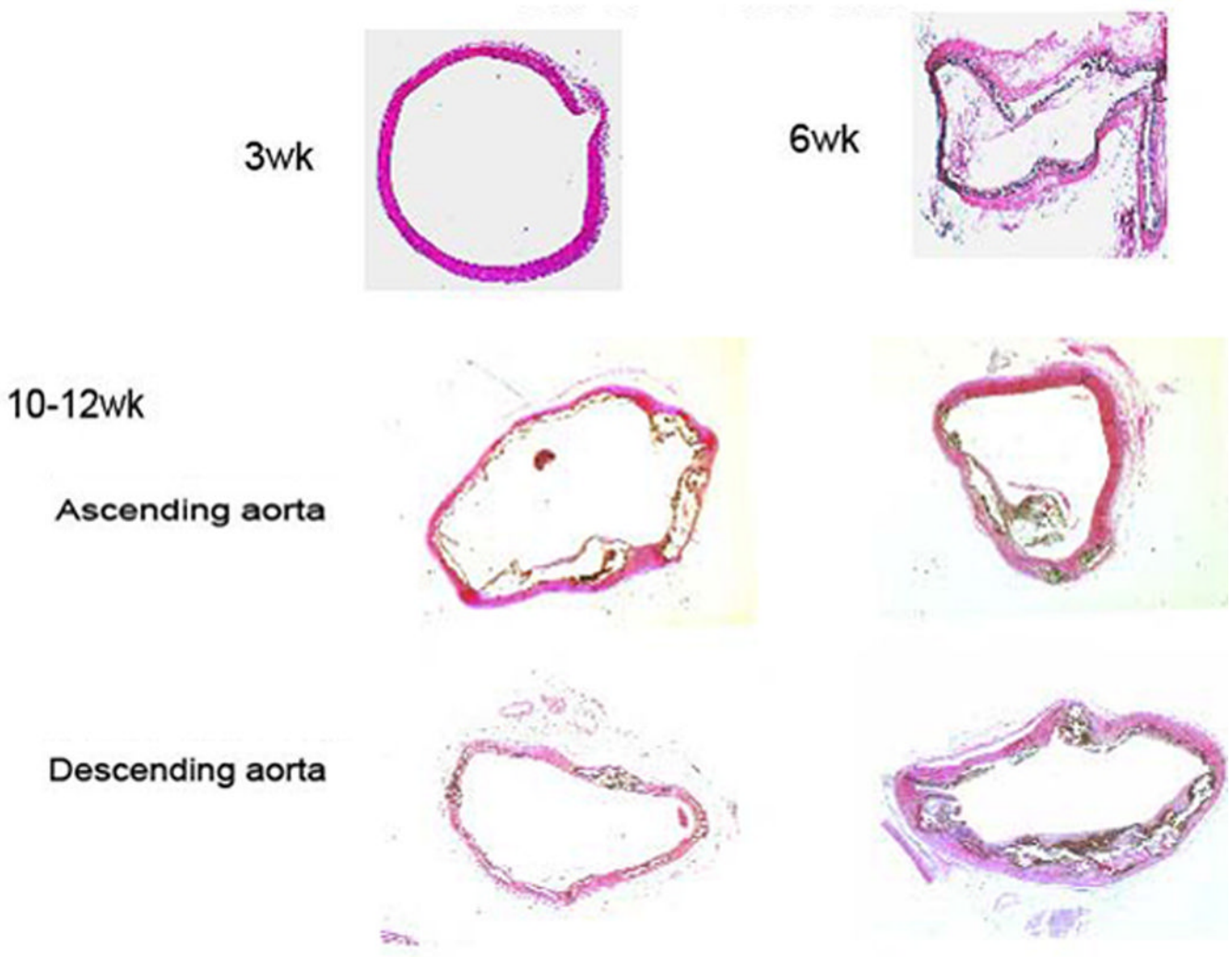

Figure 2. Cross-section of rat aortas after feeding high-fat chow

Hematoxylin and eosin staining shows calcium deposition in the ascending aorta after 6 weeks and atherosclerotic plaques were in the ascending and descending aortas after 10–12 weeks on the high fat diet.

NIH-PA Author Manuscript
NIH-PA Author Manuscript
NIH-PA Author Manuscript

Figure 3a.

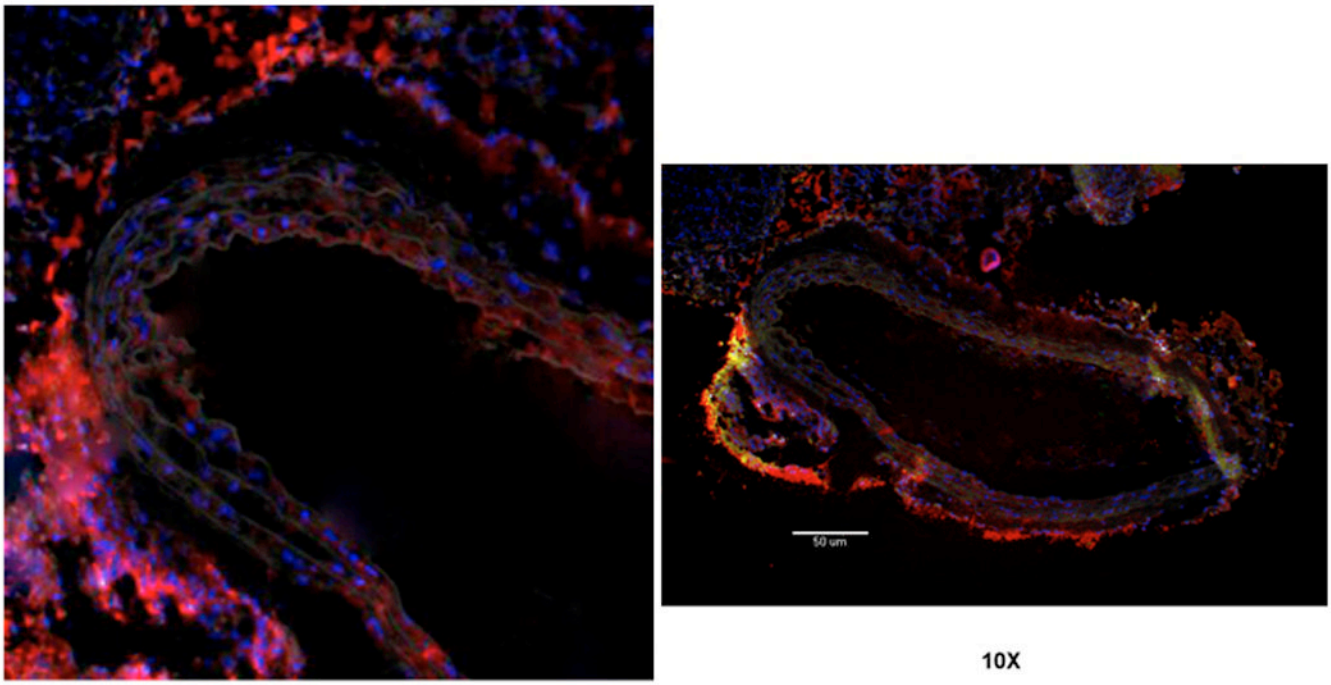

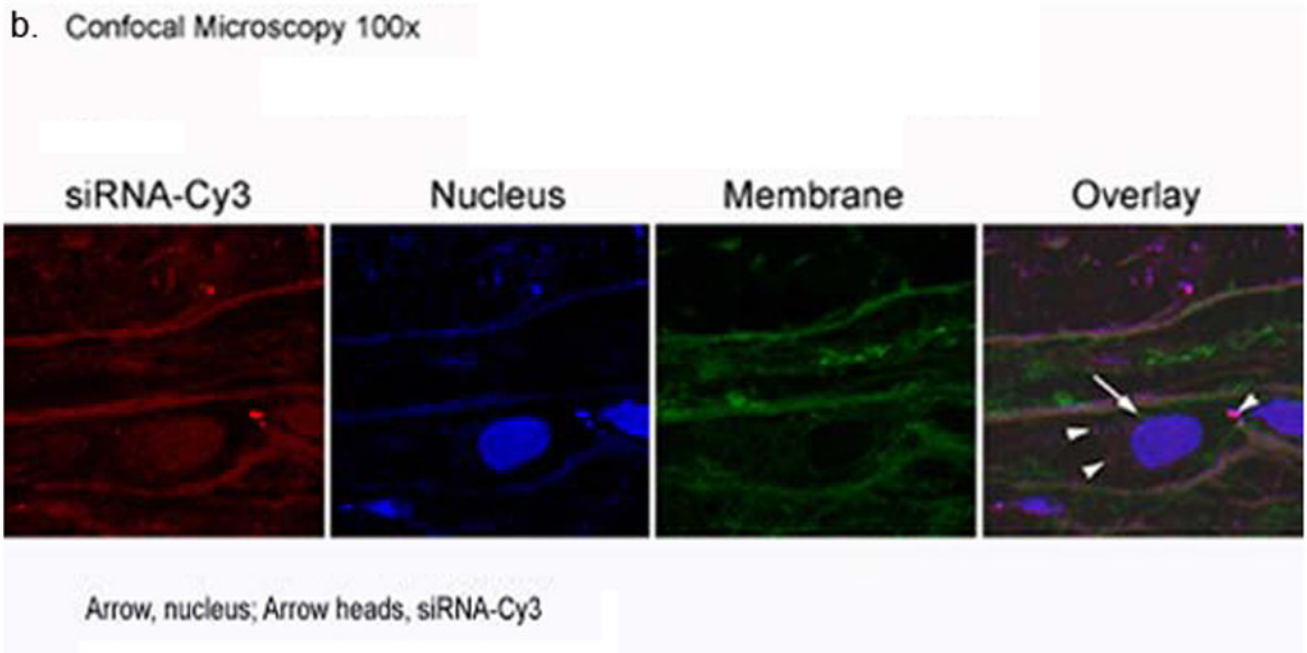

Figure 3. a,b. siGLO-nanoparticle complex transfer to the carotid artery of atherosclerotic rat

High-resolution fluorescent microscopy of left carotid artery sections harvested at four days after nanoparticle delivery of fluorescent-labeled siGLO-Dy547 (red) by local adventitia approach shows siRNA-Dy547 (siGLO, red dots) throughout the arterial wall. **Panel a**.

NIH-PA Author Manuscript

NIH-PA Author Manuscript

NIH-PA Author Manuscript

Fluorescent microscopy image. Arterial wall autoflurescence was eliminated with CRI Nuance FX multispectral imaging system and Nuance software. 10× scale bar 50μm. **Panel b**. Confocal microscopy 100× image.

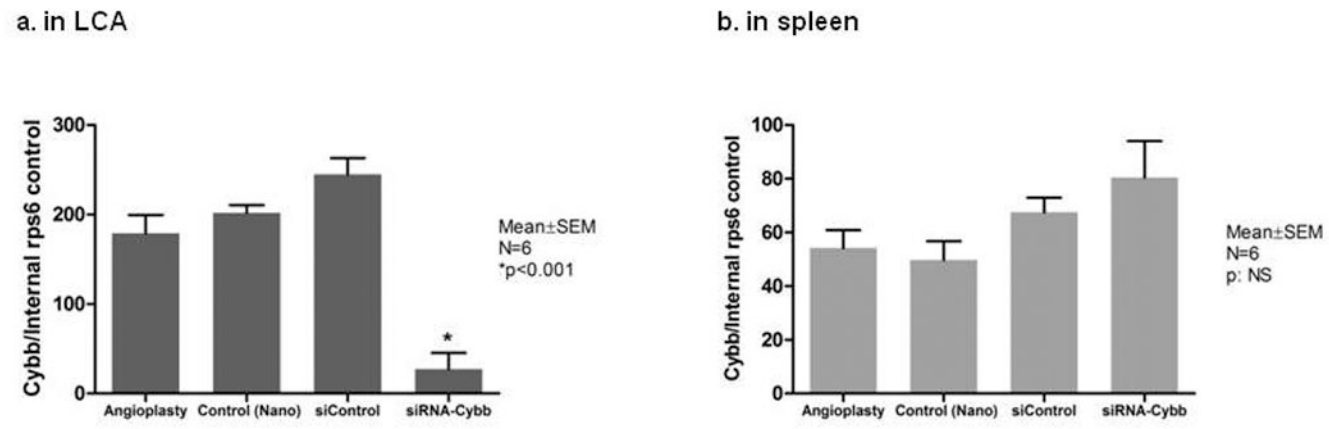

Figure 4. a,b. Cybb expression in the rat carotid artery 2 weeks after balloon angioplasty

Levels of target Cybb gene expression were determined by qRT-PCR and normalized to the internal control gene rsp6 (ribosomal protein 6). **Panel a**. Cybb expression was significantly silenced after delivery of siCybb-nanoparticle complex, compared to angioplasty alone, nanoparticle control and siControl groups. **Panel b**. No significant change in Cybb expression was found in the spleen with or without siCybb transfer. (n=6)

NIH-PA Author Manuscript
NIH-PA Author Manuscript
NIH-PA Author Manuscript

NIH-PA Author Manuscript

NIH-PA Author Manuscript

NIH-PA Author Manuscript

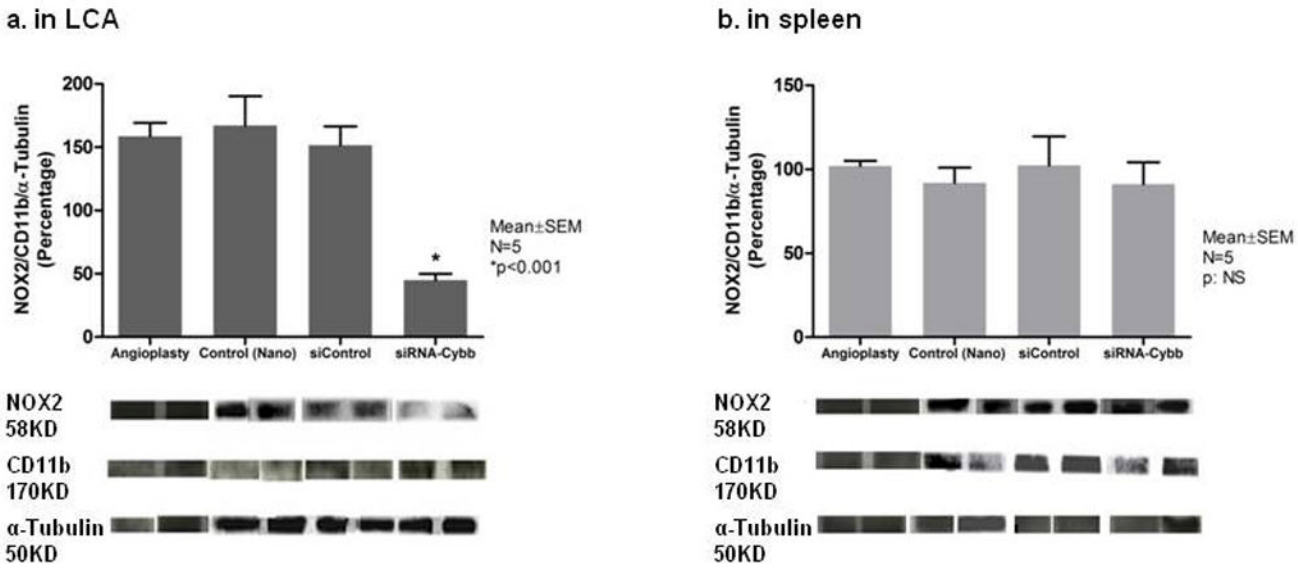

Figure 5. a,b. Western blot for NOX2 and CD11b in the rat carotid artery 2 weeks after balloon angioplasty

Panel a. NOX2 protein in the carotid artery that standardized to CD11b and α-tubulin was significantly decreased after siCybb transfer as compared to angioplasty alone, nanoparticle control and siControl groups. **Panel b**. No significant change of NOX2 protein was detected in the spleen with or without siCybb transfer. (n=5)

NIH-PA Author Manuscript

NIH-PA Author Manuscript

NIH-PA Author Manuscript

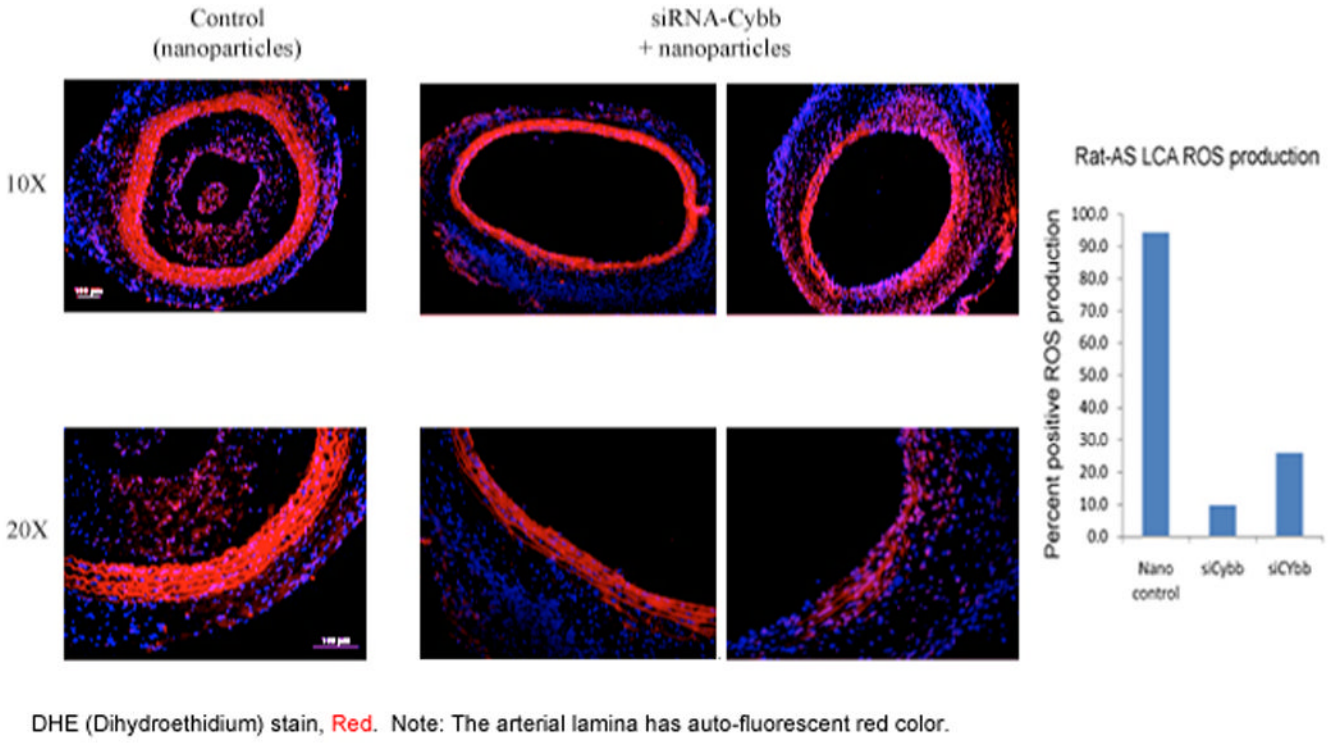

Figure 6. ROS production in rat carotid artery after angioplasty and siCybb-nanoparticle complex transfer

Carotid arteries were harvested 2 weeks after treatment and cryo-sections stained with dihydroethidium (DHE), an indicator of superoxide anions. Superoxide (red stain) is evident in thickened neointima and adventitia in the nanoparticle control group (left panel). In rat arteries treated with siCybb-nanoparticle complex (middle and right panels), neointima formation was significantly inhibited and very little superoxide is seen in the arterial wall. The far right panel graphically displays ROS in the arterial wall, quantified using IMAGE-PRO PLUS software and expressed as percent relative to the nanoparticle-only control in two experiments. Scale bar: 100μm

NIH-PA Author Manuscript
NIH-PA Author Manuscript
NIH-PA Author Manuscript

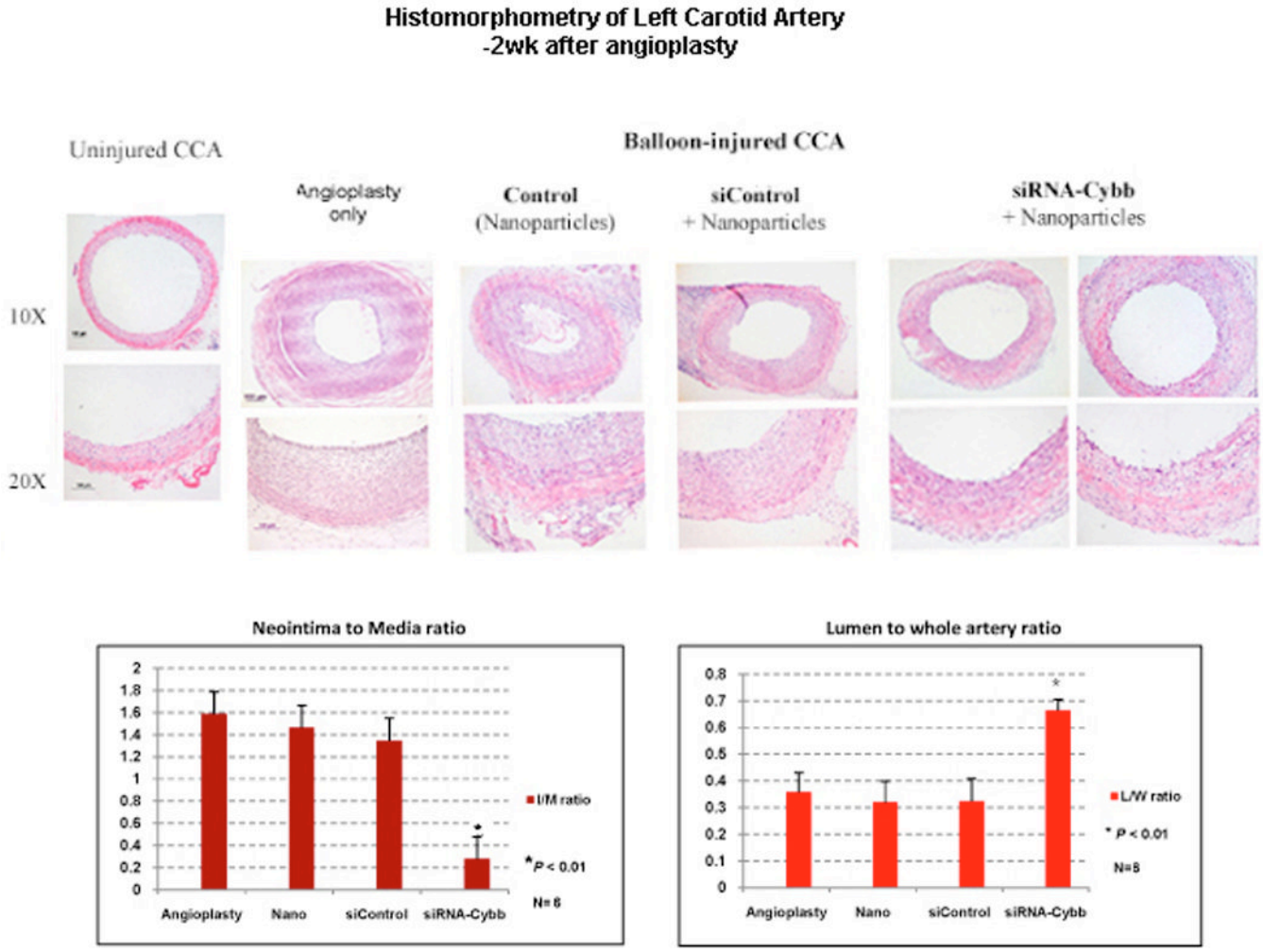

Figure 7. Neointimal and luminal area of rat carotid artery after angioplasty and siRNA-nanoparticle HB-OLD7 complex transfer

Carotid arteries were harvested 2 weeks after treatment and cryo-sections stained with hematoxylin and eosin. Neointima formation was dramatically inhibited and the arterial lumen size remarkably preserved by treatment with siCybb-HB-OLD7 complex, compared to angioplasty alone, nanoparticle control and siControl groups. (n=6) Bar graphs present quantitative measures of neointima to media (left panel) and lumen to whole artery (right panel) ratios. Scale bar: 100μm

NIH-PA Author Manuscript
NIH-PA Author Manuscript
NIH-PA Author Manuscript

Table 1

Mouse siGLO-nanoparticle complex IV organ image quantification.

	* % Positive		* % Positive		* % Positive
	1D		**3D**		**4D**
Liver	1.8	Liver	1.5	Liver	1.8
Heart	8.6	Heart	8.9	Heart	6.8
Lung	3.0	Lung	1.5	Lung	1.2
		Brain	15.7	Brain	11.6
		Spleen	15.0	Spleen	13.7
		Kidney	7.2	Kidney	6.9
		Thigh muscle	12.9		
		Leg muscle	19.9		

* Percentage of positive siGLO transferred cells to total cells.

Gene Ther. Author manuscript; available in PMC 2011 October 1.